COMPACT NOTCHED ULTRA-WIDEBAND BANDPASS FILTER WITH IMPROVED OUT-OF-BAND PERFORMANCE USING QUASI ELECTROMAGNETIC BANDGAP STRUCTURE

M.-J. Gao[*], L.-S. Wu, and J. F. Mao

Key Lab of Ministry of Education for Research of Design and EMC of High Speed Electronic Systems, Shanghai Jiao Tong University, Shanghai 200240, China

Abstract—In this paper, a compact notched ultra-wideband (UWB) bandpass filter with improved out-of-band performance using quasi electromagnetic bandgap (EBG) structure is proposed. Firstly, a UWB bandpass filter based on a stepped-impedance stub-loaded resonator (SISLR) is combined with quasi-EBG structures, which suppress the undesired spurious bands to improve the out-of-band performance. In order to eliminate the interference caused by WLAN, a notched band is introduced at 5.2 GHz, which is implemented by adding a folded stepped-impedance resonator (SIR) near the stub of the SISLR. At last, the proposed filter is fabricated and measured. Good performances of the UWB filter have been demonstrated both in the simulated and measured results.

1. INTRODUCTION

Since the U.S. Federal Communication Commission authorized the unlicensed use of ultra-wideband (UWB) with a frequency range of 3.1–10.6 GHz for commercial purposes in 2002 [1], UWB technologies have drawn much attention. As one of the essential components in UWB communication systems, the UWB bandpass filter has been rapidly developed.

In [2–8], some design methods to achieve a UWB passband have been discussed. Composite right/left-handed structures have been used to implement a UWB filter in [2] and [3]. The most popular approach to achieve the UWB response is the multiple-mode resonator (MMR)

technique, which was originally proposed in the form of a stepped-impedance resonator (SIR) in [5]. In [6] and [7], stub-loaded structures are applied to improve the in-band performance of the UWB filter, and the number of modes within the passband is increased to improve the in-band performance.

However, these structures usually have an important drawback of introducing spurious responses. Therefore, the improvement of the out-of-band performance of the UWB filter has become a research focus. The most direct method is to cascade bandpass and bandstop filters [9]. But this will lead to relatively large size. By changing the resonant modes of the MMR within the upper band, the upper stopband of the UWB filters are extended evidently [10, 11]. In [12] and [13], electromagnetic bandgap (EBG) structures are incorporated into the UWB filters to broaden the upper stopband.

Due to the existing undesired radio signals, such as WLAN, which may interfere with UWB radios, the notched band is required to reject these noises. Some solutions have been offered to generate the notch based on different theories [14–20]. In [15–17], the notched-band structures are embedded into the main body of UWB filter. And the asymmetric parallel-coupled lines can also provide a notched band [19].

To summarize, both the in-band and out-of-band performances, plus the notched band for application, should be taken into account in the design of UWB filters.

In this paper, a UWB filter with a wide upper stopband and a narrow notched band is proposed. Firstly, a stepped-impedance stub-loaded resonator (SISLR) is used to construct the main body of the UWB filter. Then, the quasi-EBG-loaded lines are introduced into SISLR, which significantly broaden the upper stopband. In order to generate a notch for WLAN, an SIR is placed near to the stub of SISLR. Good in-band and out-of-band performances of the proposed UWB filter have been demonstrated by the simulated and measured results of the filter prototype.

2. ANALYSIS AND DESIGN

2.1. Design of UWB Filter with Sharp Side Slopes

An SISLR has a structure as shown in Figure 1(a). It is composed of a traditional SIR with a stepped-impedance stub tapped-connected in the center. Since the SISLR is symmetrical in structure, the odd-/even-mode method can be used to analyze it.

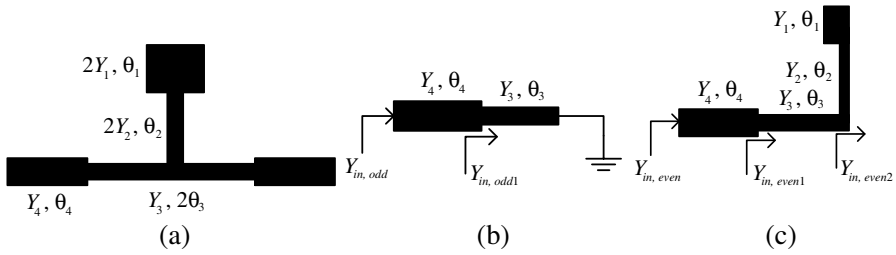For odd-mode excitation, the equivalent circuit is shown in

Figure 1. (a) Structure of an SISLR, (b) odd-mode equivalent model of SISLR, and (c) even-mode equivalent model of SISLR [7].

Figure 1(b). The resonance condition can be written as

$$Y_{in,odd} = jY_4 \frac{Y_4 \tan\theta_4 - Y_3 \cot\theta_3}{Y_4 + Y_3 \cot\theta_3 \tan\theta_4} = 0 \tag{1}$$

Then, (1) can be derived as

$$Y_4 \tan\theta_4 = Y_3 \cot\theta_3 \tag{2}$$

For even-mode excitation, the equivalent circuit is depicted in Figure 1(c). The resonance condition can be expressed as

$$Y_{in,even} = Y_4 \frac{Y_{in,even1} + jY_4 \tan\theta_4}{Y_4 + jY_{in,even1} \tan\theta_4} = 0 \tag{3}$$

where

$$Y_{in,even1} = Y_3 \frac{Y_{in,even2} + jY_3 \tan\theta_3}{Y_3 + jY_{in,even2} \tan\theta_3} \tag{4}$$

$$Y_{in,even2} = jY_2 \frac{Y_1 \tan\theta_1 + Y_2 \tan\theta_2}{Y_2 - Y_1 \tan\theta_1 \tan\theta_2} \tag{5}$$

This SISLR has several inherent transmission zeros. The frequencies of the two inherent transmission zeros located at the lower and upper cutoff frequencies are determined by the input impedance of the stub, which can be written as

$$Z_{in,even2} = 1/ (2Y_{in,even2}) = 0 \tag{6}$$

Then, we have

$$Y_2/Y_1 = \tan\theta_1 \tan\theta_2 \tag{7}$$

Based on the above analysis, by means of selecting the physical dimensions properly, a UWB filter with sharp selectivity can be achieved. Five resonant modes of SISLR are allocated within the desired UWB passband, and two transmission zeros are generated at
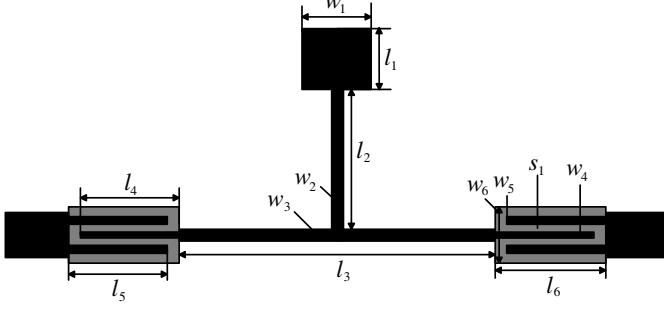
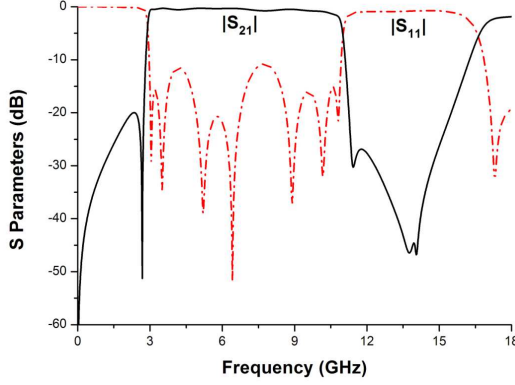**Figure 2.** Configuration of the UWB filter based on SISLR [7].

Figure 3. Simulated S-parameters of the UWB filter using SISLR.

the lower and upper band edges. To enhance the external coupling, two parallel-coupled microstrip lines are backed with apertures, as shown in Figure 2. The simulated S-parameters of the UWB filter are shown in Figure 3. The F4B substrate is used in our design, which has a relative permittivity of 2.65 and a thickness of 0.8 mm. The dimensions are optimized to be $w_1 = 3.8$, $w_2 = 0.6$, $w_3 = 1.5$, $w_4 = 0.2$, $w_5 = 0.75$, $w_6 = 3$, $l_1 = 3.6$, $l_2 = 9$, $l_3 = 15.4$, $l_4 = 7.7$, $l_5 = 7.7$, $l_6 = 8.1$ and $s_1 = 0.2$ (all in mm).

2.2. Design of UWB Filter with Improved out-of-band Performance

The configuration of the quasi-EBG-based UWB filter with improved out-of-band performance is shown in Figure 4. After substituting the middle section of the SIR of the UWB filter main body by the
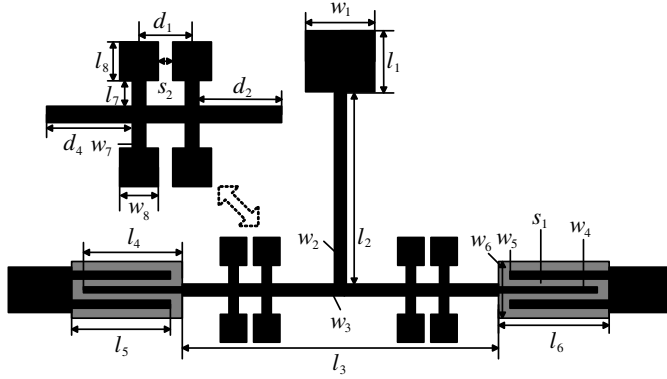
Figure 4. Configuration of the quasi-EBG-based UWB filter with improved out-of-band performance.
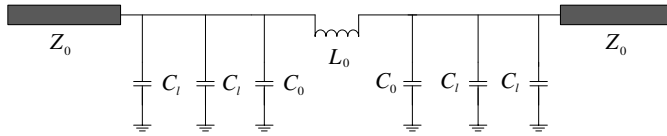

Figure 5. The equivalent circuit model of the quasi-EBG-loaded line.

quasi-EBG-loaded lines, the unwanted spurious bands can be efficiently suppressed. Quasi-EBG-loaded lines are also helpful for size reduction, due to the slow wave effect caused by the presence of the loading capacitors.

The schematic of quasi-EBG-loaded line is depicted in the inset of Figure 4, and its equivalent circuit model can be shown in Figure 5. Assuming that the transmission lines between adjacent quasi-EBG stubs can be described by the per-section inductance L_0 and capacitance C_0, and C_l represents the loaded capacitance of a single quasi-EBG stub, the cutoff frequency of the pseudo-lowpass characteristic of this structure can be given by [12]

$$f_c = \frac{1}{\pi\sqrt{L_0(C_0 + 2C_l)}} \tag{8}$$

According to the analysis of period structures with indefinite length [21], the first spurious frequency of the quasi-EBG structure, which relates to the stopband performance, can be written as

$$f_s = \frac{1}{2\sqrt{L_0 C_0}} \tag{9}$$

From (9), it is found that the stopband of the quasi-EBG-loaded lines can be set to relatively high frequencies by adjusting the dimensions properly.

Moreover, the impedance and phase shift requirements must be considered to preserve the characteristics of the original UWB filter. The equivalent characteristic impedance Z_l and phase shift φ_l of quasi-EBG-loaded line can be approximated by

$$Z_l = \frac{Z_c}{\sqrt{1 + 2C_l/C_0}} \tag{10}$$

$$\varphi_l = \varphi_0\sqrt{1 + 2C_l/C_0} \tag{11}$$

where Z_c and φ_0 are the characteristic impedance and phase shift of the unloaded microstrip line, respectively.

Figure 6 shows the simulated pseudo-lowpass characteristic of the quasi-EBG-loaded lines with different values of the gap width between two adjacent patches s_2 when the other physical dimensions are fixed and given by $w_3 = 0.7$, $w_7 = 0.4$, $w_8 = 1.6$, $l_7 = 1$, $l_8 = 1.3$, $d_1 = 1.8$, $d_2 = 1.2$ and $d_4 = 1.2$ (all in mm). After the cross coupling has been introduced between two adjacent quasi-EBG stubs, an additional transmission zero can be generated in the stopband. As a result, the stopband is extended. And it is also found in the simulated results that the distance between two transmission zeros increases with the decreasing of s_2. It's because that the narrow gap of s_2 introduces a cross coupling between two adjacent stubs, which leads to the split of the transmission zero in the stopband. The narrower the gap is, the larger the cross coupling will be. Since the lower split transmission
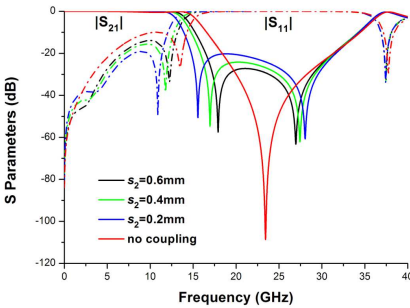

Figure 6. The pseudo-lowpass characteristic of the quasi-EBG-loaded line with different values of s_2.
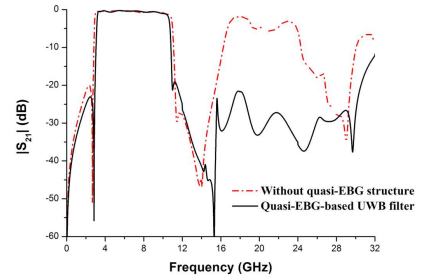
Figure 7. Comparison between the simulated transmission coefficients with and without quasi-EBG structures.

zero moves to the lower frequency side with the decrease of s_2, the cutoff frequency shifts to the lower frequency side.

Figure 7 shows the comparison between the simulated transmission coefficients with and without quasi-EBG structures. In order to maintain the good in-band performance, the dimensions are optimized to be $w_1 = 5.0$, $w_2 = 1.4$, $w_3 = 0.9$, $w_4 = 0.5$, $w_5 = 0.2$, $w_6 = 1.6$, $w_7 = 0.3$, $w_8 = 0.9$, $l_1 = 3.6$, $l_2 = 9.5$, $l_3 = 7.6$, $l_4 = 7.7$, $l_5 = 7.7$, $l_6 = 8.1$, $l_7 = 0.9$, $l_8 = 1.3$, $d_1 = 1.1$, $d_2 = 1.0$ and $s_1 = s_2 = 0.2$ (all in mm). It is also observed that the upper stopband is extended to $30.5\,\text{GHz}$ with a rejection level better than $-20\,\text{dB}$. Moreover, due to the slow wave effect of quasi-EBG-loaded lines, the filter size decreases

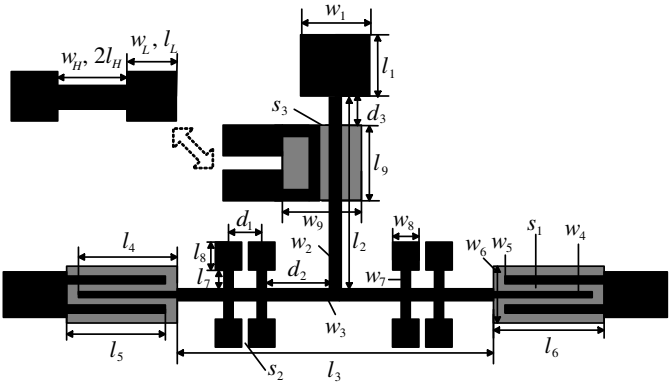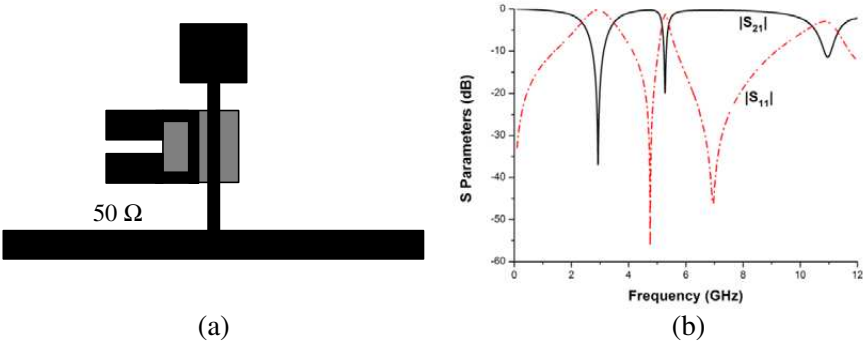**Figure 8.** Configuration of the notched UWB filter with wide upper stopband.

(a)   (b)

Figure 9. (a) The test model with a 50-Ω microstrip line loaded with the stub, and (b) the simulated results of the test model.

from $1.17 \times 0.54\lambda_0^2$ to $0.88 \times 0.59\lambda_0^2$, where λ_0 is the wavelength in dielectric at 6.85 GHz.

2.3. Notch Design

As shown in Figure 8, in order to implement a notched band within the UWB passband, a folded SIR is located near to the stub of the SISLR incorporated with quasi-EBG-loaded lines. An aperture is etched on the ground plane and just under the coupling gap so as to enhance the coupling between the folded SIR and the SISLR.

In order to explain the generating mechanism of the notch, the main body of SISLR is replaced by a 50-Ω microstrip line, as shown in Figure 9(a). From the simulated S-parameters shown in Figure 9(b), three transmission zeros are observed. The first and third ones f_{z1} and f_{z3} correspond to the transmission zeros near the lower and upper cutoff frequencies of UWB filter, respectively. Their electric field distributions are shown in Figures 10(a) and 10(b). The second one f_n is located at 5.27 GHz, and the simulated electric field distribution at this frequency has been illustrated in Figure 10(c). It is found that the electric field reaches its minimum at the loading point for all frequencies
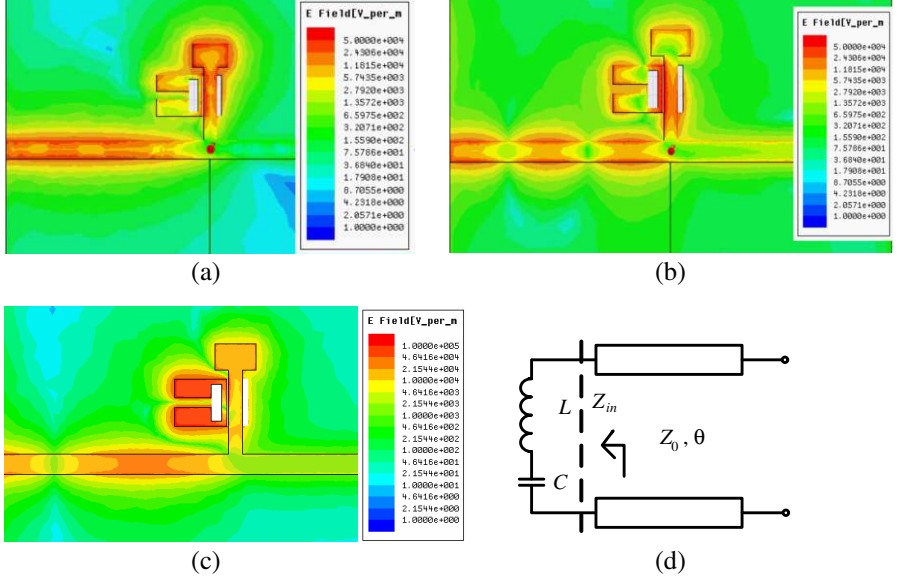

(a)

(b)

(c)

(d)

Figure 10. The electric field distributions of the test model for (a) f_{z1}, (b) f_{z3}, and (c) f_n, and (d) the approximate model for the explanation of the second transmission zero.

of the transmission zeros, which means the notch also satisfies (6).

To ensure the notch is located at the desired WLAN frequency, the resonance condition of the SIR should be considered carefully. In order to explain this problem simply, the stepped-impedance stub is replaced by a uniform-impedance one approximately. The simplified circuit model is shown in Figure 10(d). Then, the input impedance of the resonator can be expressed like a series resonant circuit, i.e.,

$$Z_{in} = j\omega L + \frac{1}{j\omega C} = j\omega_0 L \left(\frac{\omega}{\omega_0} - \frac{\omega_0}{\omega} \right) \tag{12}$$

where L and C are the equivalent inductance and capacitance of the folded SIR, respectively. And note that $\omega_0 = 1/\sqrt{LC}$ is the resonant frequency of the SIR. Based on (6) and Figure 10(d), the notch will arise when

$$\tan \theta_n = \frac{1/(\omega_n C) - \omega_n L}{Z_0} \tag{13}$$

where Z_0 and θ_n are the characteristic impedance and electrical length of the approximate uniform-impedance stub at the notch frequency, respectively.

If $\omega_n \geq \omega_0$, we should have $\pi/2 < \theta_n < \pi$ and the notch frequency f_n satisfies $1 < f_n/f_{z1} < 2$. If $\omega_n \leq \omega_0$, we have $\pi < \theta_n < 3\pi/2$ and then the notch frequency f_n would be more than twice of the frequency f_{z1} of the first transmission zero. In our design, the first transmission zero is set to about 3.0 GHz and the notch frequency is desired at 5.2 GHz. Therefore, the resonant frequency of the SIR should satisfy $\omega_n \geq \omega_0$. The dimensions of the folded SIR are $w_L = 2$, $w_H = 0.5$, $l_L = 3.9$ and $l_H = 3.7$ (all in mm). Its resonant frequency 4.8 GHz is below the notched band, and the notch can be achieved around 5.2 GHz successfully.
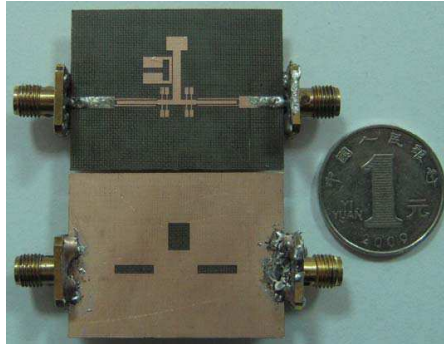

Figure 11. Photo of the fabricated UWB filter prototype.

3. RESULTS AND DISCUSSION

To validate our design, the proposed notched UWB filter is fabricated on a F4B substrate, as shown in Figure 11. The dimensions are optimized with the commercial software, Ansoft HFSS, and given by $w_1 = 4.8$, $w_2 = 1.5$, $w_3 = 0.8$, $w_4 = 0.5$, $w_5 = 0.2$, $w_6 = 1.6$, $w_7 = 0.3$, $w_8 = 0.7$, $w_9 = 4$, $l_1 = 2.8$, $l_2 = 9$, $l_3 = 7.1$, $l_4 = 7.7$, $l_5 = 7.7$, $l_6 = 8.1$, $l_7 = 1.1$, $l_8 = 1.3$, $l_9 = 5$, $d_1 = 0.9$, $d_2 = 1$, $d_3 = 1$, $s_1 = 0.2$ and $s_2 = 0.2$ (all in mm). The overall size of the fabricated filter prototype is about $0.87 \times 0.54 \lambda_0^2$.

Figure 12 shows the simulated and measured results of the proposed filter, where reasonable agreement can be observed. Due to fabrication tolerance, there are some slight discrepancies between them. The transmission zero near the upper band edge is not as obvious as that of the UWB filter without notch, which can be seen both in the simulated and measured results. The reason is that the

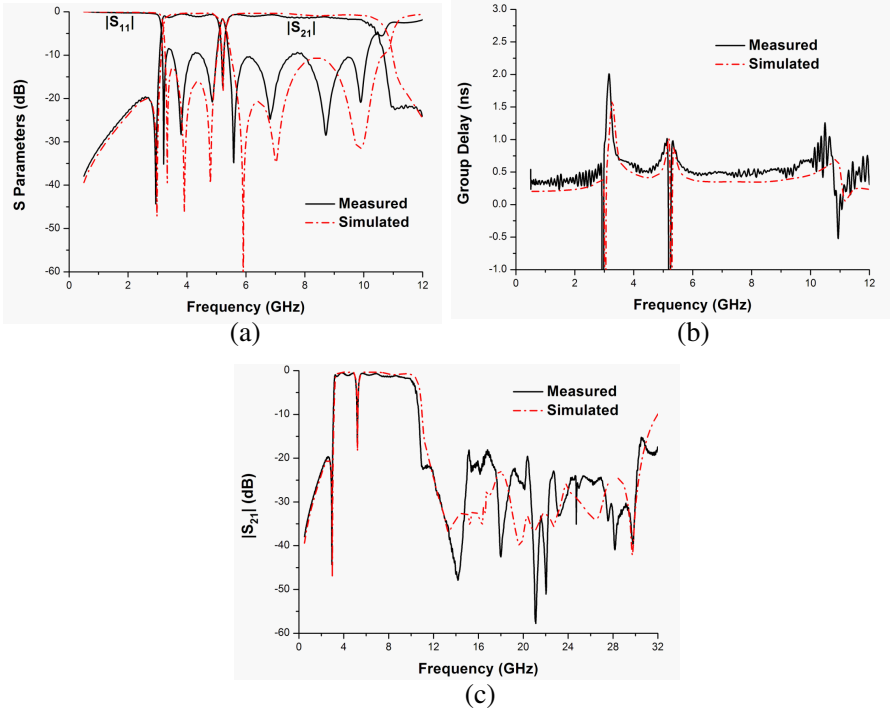

Figure 12. (a) Simulated and measured S-parameters from 0.5 to 12 GHz of the filter prototype, (b) its simulated and measured group delays from 0.5 to 12 GHz, and (c) the simulated and measured transmission coefficients from 0.5 to 32 GHz.

folded SIR and the aperture on the ground will introduce more loss at high frequency range and degrade the performance.

According to the measured results, the UWB filter has a 10 dB passband from 3.07 to 10.69 GHz. The notched band is measured from 5.17 to 5.25 GHz with −10 dB rejection. And the insertion loss is measured less than −1.7 dB within the passband. The measured in-band return loss is mostly better than −10 dB. And the measured group delay is flat within its passband, as shown in Figure 12(b). Its response within a wide frequency range is shown in Figure 12(c), from which it is seen that the measured upper stopband has been improved up to 30.4 GHz, with a rejection level better than −18 dB.

The comparison between the performances of previously published UWB filters and our proposed one is summarized in Table 1. Due to the two transmission zeros located at the lower and upper band edges, which are generated by the stepped-impedance stub in the center, good frequency selectivity is achieved. By using quasi-EBG-loaded lines, our proposed UWB filter has good out-of-band rejection performance. By properly loading a folded SIR, a notch is generated within the UWB passband, without significantly increasing the occupied area. Therefore, all the performances of UWB passband, sharp side slopes, wide upper stopband and a narrow notched band have been realized with a compact size.

Table 1. Comparison between the performances of previous UWB filters and the proposed UWB filter.

Ref.	IL (dB)	FCC UWB Passband	Frequency Selectivity	f_c (GHz)	f_n (GHz)	Size $(\lambda_0 \times \lambda_0)$
[5]	≤ 2.0	Yes	Normal	13.8	- -	1.22×0.14
[6]	≤ 1.4	Yes	Normal	15.8	- -	1.05×0.23
[7]	≤ 2.5	Yes	Good	16.1	- -	1.19×0.57
[10]	≤ 1.1	Yes	Normal	26.7	- -	0.71×0.52
[12]	≤ 0.9	No	Normal	22.8	- -	1.19×0.84
[16]	≤ 0.7	Yes	Normal	15.5	5.8	0.89×0.60
[17]	≤ 0.5	Yes	Good	14.8	5.4/6.1	0.37×0.30
[19]	≤ 1.0	Yes	Normal	14.5	6.6	1.20×0.14
This work	≤ 1.7	Yes	Good	30.4	5.2	0.87×0.54

IL means in-band insertion loss, f_c is the upper stopband frequency with an −18-dB rejection, f_n is the notch frequency, and λ_0 is the wavelength in dielectric at 6.85 GHz.

4. CONCLUSION

A compact UWB filter with wide upper stopband and a narrow notched band is proposed in this paper. The main body of the filter is constructed by an SISLR. The transmission poles and zeros are properly located in the passband and band edges, respectively. As a result, good frequency selectivity is achieved for the UWB filter. In order to extend the upper stopband, the quasi-EBG-loaded lines are introduced into the SISLR to provide the pseudo-lowpass characteristic, which significantly broaden the upper stopband. In order to generate a notch for WLAN, a folded SIR is placed near to the stub of SISLR. Good in-band and out-of-band performances of the proposed UWB filter have been demonstrated by the simulated and measured results of the filter prototype.

REFERENCES

1. "Revision of Part 15 of the commission's rules regarding ultra-wideband transmission system," ET-Docket 98-153, First note and order, Federal Communication Commission, Feb. 14, 2002.
2. Chou, T.-C., M.-H. Tsai, and C.-Y. Chen, "A low insertion loss and high selectivity UWB bandpass filter using composite right/left-handed material," *Progress In Electromagnetics Research C*, Vol. 17, 163–172, 2010.
3. Huang, J.-Q. and Q.-X. Chu, "Compact UWB band-pass filter utilizing modified composite right/left-handed structure with cross coupling," *Progress In Electromagnetics Research*, Vol. 107, 179–186, 2010.
4. Yang, G., W. Kang, and H. Wang, "An UWB bandpass filter based on single ring resonator and shorted stubs loaded without coupled feed lines," *Journal of Electromagnetic Waves and Applications*, Vol. 25, No. 16, 2159–2167, 2011.
5. Zhu, L., S. Sun, and W. Menzel, "Ultra-wideband (UWB) bandpass filter using multiple-mode resonator," *IEEE Microw. Wireless Compon. Lett.*, Vol. 15, No. 11, 796–798, Nov. 2005.

6. Li, R. and L. Zhu, "Compact UWB bandpass filters using stub-loaded multiple-mode resonator," *IEEE Microw. Wireless Compon. Lett.*, Vol. 17, No. 1, 40–42, Jan. 2007.

7. Chu, Q.-X. and X.-K. Tian, "Design of UWB bandpass filter using stepped-impedance stub-loaded resonator," *IEEE Microw. Wireless Compon. Lett.*, Vol. 20, No. 9, 501–503, Sep. 2010.

8. Fallahzadeh, S. and M. Tayarani, "A new microstrip UWB bandpass filter using defected microstrip structures," *Journal of Electromagnetic Waves and Applications*, Vol. 24, No. 7, 893–902, 2010.

9. Tang, C.-W. and M.-G. Chen, "A microstrip ultra-wideband bandpass filter with cascaded broadband bandpass and bandstop filters," *IEEE Trans. Microw. Theory Tech.*, Vol. 55, No. 11, 2412–2418, Nov. 2007.

10. Wong, S.-W. and L. Zhu, "Quadruple-mode UWB bandpass filter with improved out-of-band rejection," *IEEE Microw. Wireless Compon. Lett.*, Vol. 19, No. 3, 152–154, Mar. 2009.

11. Deng, H.-W., Y.-J. Zhao, X.-S. Zhang, L. Zhang, and S.-P. Gao, "Compact quintuple-mode UWB bandpass filter with good out-of-band rejection," *Progress In Electromagnetics Research Letters*, Vol. 14, 111–117, 2010.

12. Garcia-Garcia, J., J. Bonache, and F. Martin, "Application of electromagnetic bandgaps to the design of ultra-wide bandpass filters with good out-of-band performance," *IEEE Trans. Microw. Theory Tech.*, Vol. 54, No. 12, 4136–4140, Dec. 2006.

13. Wong, S.-W. and L. Zhu, "EBG-embedded multiple-mode resonator for UWB bandpass filter with improved upper-stopband performance," *IEEE Microw. Wireless Compon. Lett.*, Vol. 17, No. 6, 421–423, Jun. 2007.

14. Chu, H. and X. Q. Shi, "Compact ultra-wideband bandpass filter based on SIW and DGS technology with a notch band," *Journal of Electromagnetic Waves and Applications*, Vol. 25, No. 4, 589–596, 2011.

15. Xu, J., B. Li, H. Wang, C. Miao, and W. Wu, "Compact UWB bandpass filter with multiple ultra narrow notched bands," *Journal of Electromagnetic Waves and Applications*, Vol. 25, No. 7, 987–998, 2011.

16. Shaman, H. and J.-S. Hong, "Ultra-wideband (UWB) bandpass filter with embedded band notch structures," *IEEE Microw. Wireless Compon. Lett.*, Vol. 17, No. 3, 193–195, Mar. 2007.

17. Huang, J.-Q., Q.-X. Chu, and C.-Y. Liu, "Compact UWB filter based on surface-coupled structure with dual notched bands," *Progress In Electromagnetics Research*, Vol. 106, 311–319, 2010.

18. Liu, C.-Y., T. Jiang, and Y.-S. Li, "A novel UWB filter with notch-band characteristic using radial-UIR/SIR loaded stub resonators," *Journal of Electromagnetic Waves and Applications*, Vol. 25, Nos. 2–3, 233–245, 2011.

19. Shaman, H. and J.-S. Hong, "Asymmetric parallel-coupled lines for notch implementation in UWB filters," *IEEE Microw. Wireless Compon. Lett.*, Vol. 17, No. 7, 516–518, Jul. 2007.

20. Chu, H., X. Q. Shi, and Y. X. Guo, "Ultra-wideband bandpass filter with a notch band using EBG array etched ground," *Journal of Electromagnetic Waves and Applications*, Vol. 25, Nos. 2–3, 203–209, 2011.

21. Pozar, D. M., *Microwave Engineering*, Wiley, New York, 1998.